

Steel Collar Strengthening of a Slab-Column Connection under Eccentric Load

Hanaa Abdulbaset Ali

Department of Civil Engineering, University of Baghdad, Iraq
hanaa.ali2001d@coeng.uobaghdad.edu.iq (corresponding author)

Mohannad H. Al-Sherrawi

Department of Civil Engineering, University of Baghdad, Iraq
Dr.Mohannad.Al-Sherrawi@coeng.uobaghdad.edu.iq

Received: 31 March 2024 | Revised: 20 April 2024 and 22 April 2024 | Accepted: 23 April 2024

Licensed under a CC-BY 4.0 license | Copyright (c) by the authors | DOI: <https://doi.org/10.48084/etasr.7391>

ABSTRACT

The current study focuses on the punching shear resistance of reinforced concrete flat slabs with steel collars, examining it both experimentally and numerically. Six square flat slab specimens were casted and tested under static load, axial load, and eccentric load. The effects of the steel collars and eccentricity on the load-displacement behavior, ultimate load capacity, cracking load, failure mode, stiffness, failure angle, and ductility, were investigated. The results demonstrated that using steel collars in slab-column connection greatly increases the shear capacity of the slab under eccentric loads and moments. The strengthened slabs' ultimate capacity increased by 34% and 61%, respectively, compared to that of the slabs without collars. ABAQUS simulation results were in good accordance with the experiments. The findings underline the efficiency of the steel collars in increasing the efficiency of slab-column connections with punching shear, which is a cost-effective strengthening technique. This research provides knowledge about slab-column connections and offers relevant indications for the design and strengthening of the construction.

Keywords-slab-column connection ; flat slab; steel collar

I. INTRODUCTION

Reinforced concrete flat slab systems, characterized by their uniform slab thickness directly supported by columns, offer numerous advantages, such as reduced construction time, cost-effective formwork, increased building height efficiency, and enhanced architectural design flexibility [1-3]. However, one critical challenge associated with flat slab systems is the danger of punching shear collapse at the slab-column connection due to the transfer of shear forces and unbalanced moments. This failure occurs when the column and a fraction of the slab are pushed together by the slab's vertical loads and transmitted moments, particularly at the edge and corner regions of the connection [4-6]. Various strengthening techniques, including steel plates, steel bolts, and Fiber-Reinforced Polymers (FRP) [7-10], have been proposed and experimentally studied to mitigate this problem and enhance the structural performance of the flat slab systems. These methods aim to improve the slab-column connections' bearing stress and punching shear capacity. Experimental studies have investigated the effectiveness of these strengthening techniques, particularly of the steel collars, and highlighted their positive impact on punching shear capacity [11-13]. Researchers have recently explored the application of steel collars as an alternative strengthening method for slab-column connections. Steel collars offer unique advantages in terms of both ease of

implementation and cost-effectiveness. They have shown significant potential in increasing the shear strength and load resistance of slabs subjected to eccentric loads and unbalanced moments [14, 15]. However, the available literature primarily focuses on concentrated load effects, and there is limited knowledge about the behavior of steel collar strengthening under eccentric loading conditions [16-20].

This study aims to investigate the effect of steel collars and eccentric load on the punching shear strength of flat slabs. The experimental program involves testing six solid slab specimens, considering various eccentric load configurations and the presence of steel collars. The ultimate load capacity, load-displacement behavior, failure mode, stiffness, and failure angle of the slab-column connection will be evaluated and compared. A finite element analysis using the ABAQUS software will be conducted to validate the experimental findings and provide further insights into the behavior of the strengthened slab-column connections. The remainder of this study provides the study methodology, including the dimensions of the test specimens and the details of the steel collar strengthening technique and presents the experimental and numerical test results as well as a discussion and conclusions, entailing key insights, recommendations for future research, and practical implications.

II. MATERIALS AND METHODS

A. The Model Scale of the Studied Flat Slab

The prototype structure employed in this study, as depicted in Figure 1, was a flat plate floor system supported by columns with a 7.0 m span in both directions and a 200 mm total slab thickness. To represent a simply supported isolated flat plate specimen, an apportion of the interior slab around the slab-column connection, enveloped by lines of contra-flexure or inflection point (zero moments), can be taken where the distance between the contra-flexure points represents the dimensions of the specimens. Figure 2 illustrates a moment diagram around contra-flexure points. The (x) value equals to 0.211 L and was determined by finding the zero moment point of the one span fixed end supports.

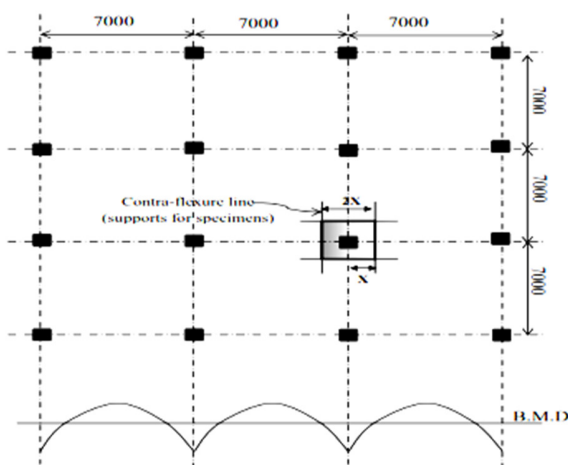


Fig. 1. Prototype of the flat slab.

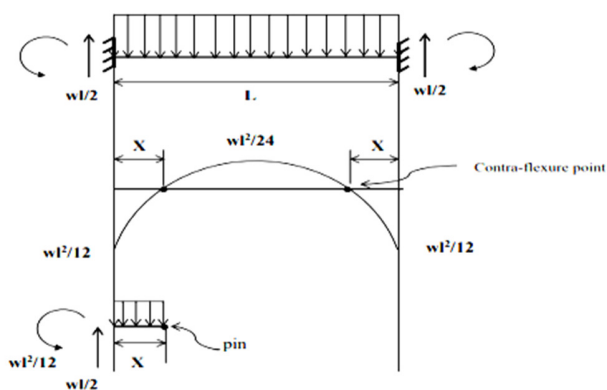


Fig. 2. Bending moment diagram of one floor of the structure.

The test specimens' dimensions were 2900×2900 mm, depending on the previous explanation. Considering the total cost and laboratory facilities, the half-scale was finally selected, making all test specimens to have dimensions of 1400×1400 mm and 100 mm overall thickness, whereas the and column stubs has dimensions of 150×150 mm in the center of the slab with a height of 200 mm.

B. Description of Flat Slab Specimens

The experimental program includes testing six 1400×1400×100 mm solid slabs with 1300 mm effective span to assess the eccentric load and steel collar effects. SC₁ refers to the flat slab with load at the center of the column, SC₂ and SC₃ with $e_1 = 100$ mm and $e_2 = 150$ mm load applied from the center, with s referring to the steel collar used. Table I portrays the details of the slabs. The slab steel reinforcement layout is the same for all testing specimens. The tension side of the test specimens was reinforced with $\phi 10$ mm bars at 75 mm in both directions, which corresponds to (1.45%) reinforcement ratio. The compression side was reinforced with $\phi 8$ mm bars at 150 mm in both directions, which corresponds to 0.43% reinforcement ratio as observed in Figure 3. The reinforcement in the stub column consists of four 16 mm bars enclosed by two $\phi 8$ mm ties.

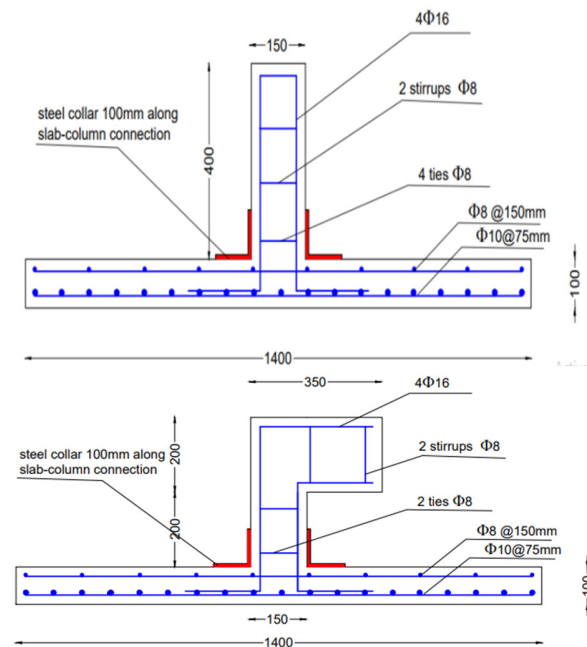


Fig. 3. Steel reinforcement of flat slabs.

Slab-column connections were strengthened with a 6 mm thickness steel collar of four angles, a part of the column cut with 90° and slab cutting with 135°. The yielding stress of the steel was 445 MPa. The concrete area where the steel angle would be installed underwent roughening and cleaning procedures. Subsequently, the steel angles were attached to the concrete using epoxy resin and were securely tightened on all four sides of the column. The four steel plates (steel angles) were welded together to form a collar at the corners around the slab-column connection. The critical section for a two-way member without shear reinforcement formed a rectangular perimeter b_o around the column located at $d/2$ from the face of the column following ACI Code 318 [21], as noticed in Figure 4.

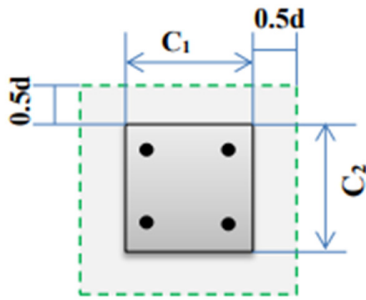


Fig. 4. Critical slab section without shear reinforcement for punching shear.

The concrete mix was obtained from the trial mixes utilizing Portland cement type I. Coarse aggregate with maximum size of 12 mm was deployed, along with fine sand, 0.42% super-plasticizer, 0.47 water/cement ratio, and C:S:G of 1:1.75:2.47. For the experiments, according to ASTM C39/C39M21 and ASTM C496/C496M-17, three 150×300 mm concrete cylinders were cast and tested to measure the splitting tensile strength (f_t), and compressive strength (f_c'), respectively [22, 23], and three prisms (400×100×100 mm) were tested according to ASTM C78/C78M-21 [24] to find the concrete modulus of rupture (f_r).

All specimens were cast and cured the same way. After 28 days, the hardened concrete was tested for modulus of rupture, compressive strength, and splitting tensile strength. The modulus of elasticity was calculated by the ACI 318-19 equation: ($E_c = 4700 \sqrt{f_c}$). Table II shows the results of the average strength of the set three specimens for all tests.

III. TEST SETUP

All simply supported specimens were tested until failure under static load (eccentric and concentrated). The load applied was transferred from the column to the slabs [25-28]. At the beginning of the test, all slabs were prepared and set at a suitable place, and the supports were located on the four sides by a steel frame. The load was applied on the slab on the column face and instrumented according the load cells, strain gauges, and Linear Variable Displacement Transducer (LVDT). After setting the studied slab specimen on the testing frame, all LVDTs, load cell readings, and strain gauges were calibrated to zero. Throughout the loading process, the crack appearance and development were observed first on the high-tension surfaces and later on the compression surfaces of the specimens. Punched zone perimeter, area, and punching angle were measured when the specimen slab collapsed. Figure 5 showcases the testing instrument.

TABLE I. DETAILS OF FLAT SLABS

Specimen group	Specimen designation	Parameter studied	Steel collar length	Steel collar thickness	Eccentricity from the center	Moment
I	SC1	Values of applied moment	-	-	At the center	-
	SC2				e_1	$P \times e_1$
	SC3				e_2	$P \times e_2$
II	SC1s1	Values of applied moment	L_1	t_1	At the center	-
	SC2s1				e_1	$P \times e_1$
	SC3s1				e_2	$P \times e_2$
III	SC2	Geometry of steel collar	-	-	e_1	$P \times e_1$
	SC2s1		L_1	t_1		$P \times e_1$
IV	SC3	Geometry of steel collar	-	-	e_2	$P \times e_2$
	SC3s1		L_1	t_1		$P \times e_2$

*I,II- group number, S- flat slab C- column ,s-steel collar, P- ultimate load, e- eccentricity, M- moment

TABLE II. CONCRETE STRENGTH RESULTS

Slab ID	Cylinder strength f_c' , MPa	Splitting tensile strength f_t , MPa	Modulus of rupture f_r , MPa	Modulus of elasticity E_c , MPa
SC1, SC2, SC3, SC1s1, SC2s1, SC3s1	33.4	3.22	3.12	25254



(a)



(b)

Fig. 5. Testing slabs.

IV. RESULTS AND DISCUSSION

A. Failure Modes of Slabs

Most unstrengthened specimens tested in this study failed suddenly to punch shear in the slabs, whereas the strengthened specimens with steel collars failed gradually under the effect of either concentrated or eccentric load. The flat slabs reached failure step by step with increased cracks that expand from the critical area towards the edges and the center, forming an X-shape with the increment of load. The first cracks on the slab bottom surfaces at most slabs appeared at the same load level, whereas the cracks on the top slab surfaces occurred when the columns punched the slabs at maximum load. The cracks took place in a circular shape when the steel collar was not used. For the plates strengthened with steel collars, the crack patterns occur in a rectangular form and increase the ductility of failure. The eccentric load applied on the column led to the punching failure occurring on three sides, directly at the compression side. However, the crack patterns were smaller on the tension side, so the failure mode became less brittle. Figure 6 illustrates the failure modes of the tested slabs.

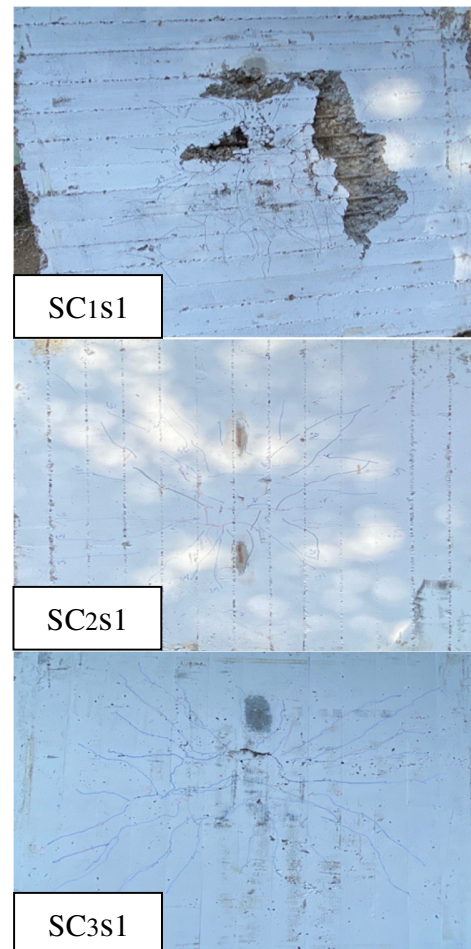
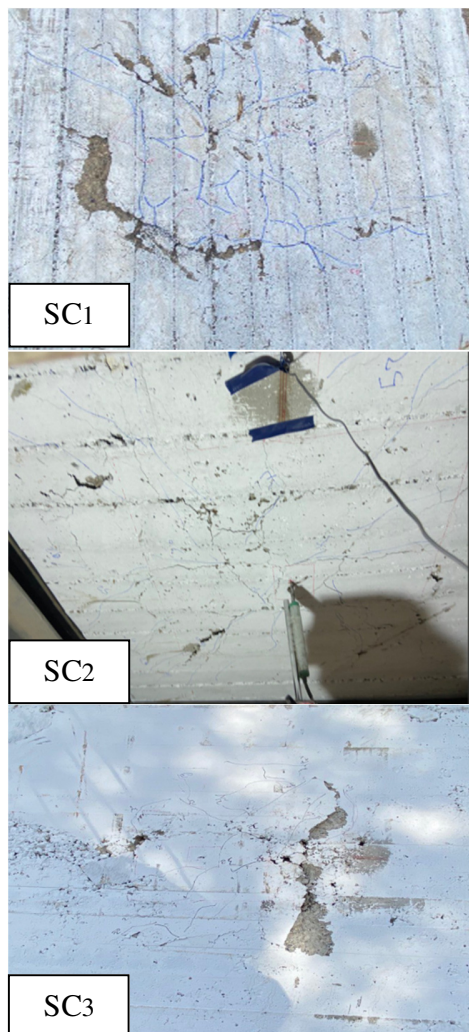


Fig. 6. Failure modes of the slabs.

B. Load-Deflection

Figure 7 portrays the load-deflection relationship of the construction member at the limit state of the slab. The behavior of the tested slabs with $e = 100$ mm and 150 mm (SC2 and SC3 group I) displayed a decrease in load compared to the reference specimen SC1, whereas group II manifested effective strengthening (by the steel collar) of the region of slab-column connection. Specimens SC1s1, SC2s1, and SC3s1 exhibited an increased maximum load level compared to group I by 26%, 34%, and 61%, respectively. Groups III and IV gave 34% and 65% improvement in the ultimate load, when it was applied with the same eccentricity, but by using steel collars in SC2s1 and SC3s1. The crack load slightly differs from one specimen to another. Table III provides the experimental results.

V. FINITE ELEMENT ANALYSIS AND MODELING OF THE FLAT SLABS

ABAQUS/ CAE 6.14 was employed to analyze all tested slabs and model concrete, steel reinforcements, and steel collars. The Finite Element Method (FEM) elucidates the application of reinforced concrete elements, the modeling of concrete under tension, and the analysis of the axial compression of the state stresses. The performance of the crack pattern model was also depicted.

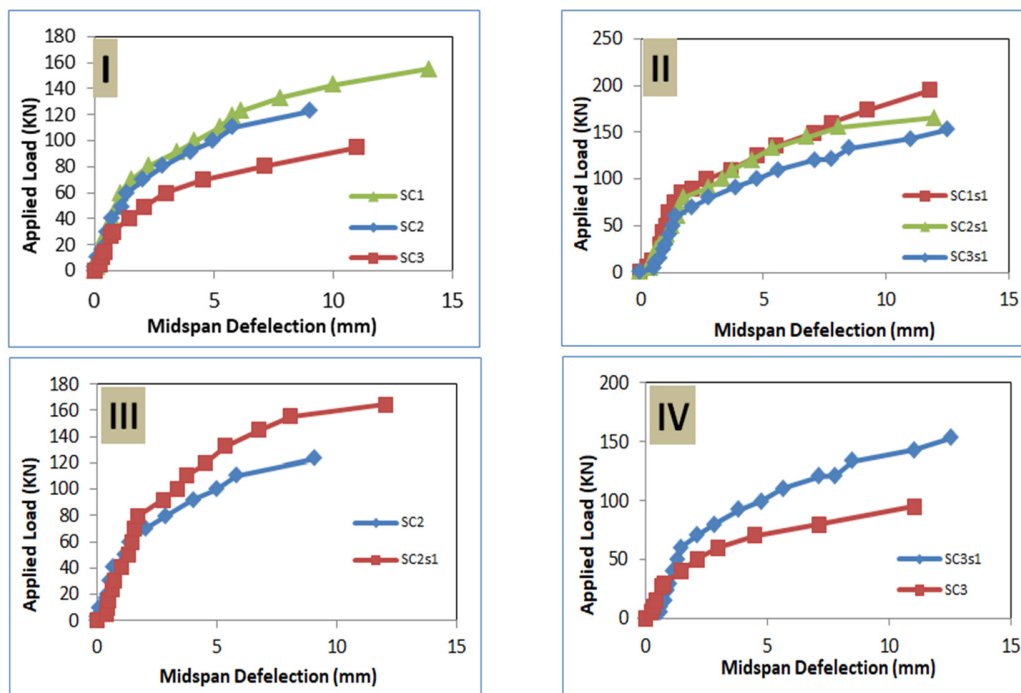


Fig. 7. Testing slab results.

TABLE III. RESULT SUMMARY

Specimen ID	P_{cr} (kN)	Δ_{cr}	P_u (kN)	Δu (mm)	Perimeter of failure area (mm)	Angle of failure	Enhancement ratio of P_u (%)
SC ₁	32	1.25	155	12.5	2650	13.5	Reference
SC ₂	30	2.2	123	10	1540	11.5	Reference
SC ₃	24	2.1	95	9	1210	10	Reference
SC _{1s1}	35	1.8	196	12	2850	17.5	26
SC _{2s1}	31	2.4	165	13	2630	15.2	34
SC _{3s1}	32	2.1	153	12.5	2115	13.2	61

To model the material, three-dimensional elements with three degrees of freedom in the directions x, y, and z for each node, were utilized. Figures 8, 9, and 10 show the concrete mesh, the steel mesh, and the steel collars, respectively. Eight nodes (13120 linear hexahedral elements of type C3D8R) were put into service for the brick element, two (1634 linear element of type T3D2) nodes were engaged for the truss element, and four (256 linear quadrilaterals of type S4R) nodes were used for the shell element. The concentrated load was simulated with 13542 linear hexahedral elements of type C3D8R, 1652 linear elements of type T3D2, and the eccentric load with 454 linear quadrilateral of type S4R. Specimens with dimensions of 1400×1400×100 mm were considered throughout the simulation analysis of all tested samples. The boundary conditions for model displacement were subjected to simple supports along the whole edge length of the simulated slab, just like the tested ones. The steel plate, which was placed on the column to apply load on it, was simulated in ABAQUS adopting the same approach as that followed in the experimental work. The load was evenly transversed across all nodes situated on the extreme surface of the column. The system was simulated as a load control implementing finite element models to achieve a state of equilibrium by balancing the internal forces. The value of the load increment was 10 kN.

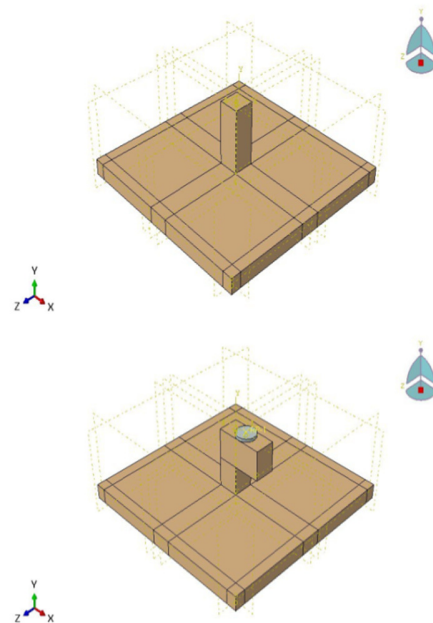


Fig. 8. Concrete mesh.

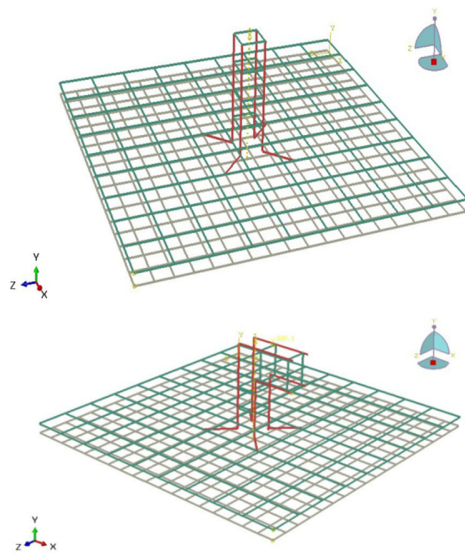


Fig. 9. Steel reinforced mesh.

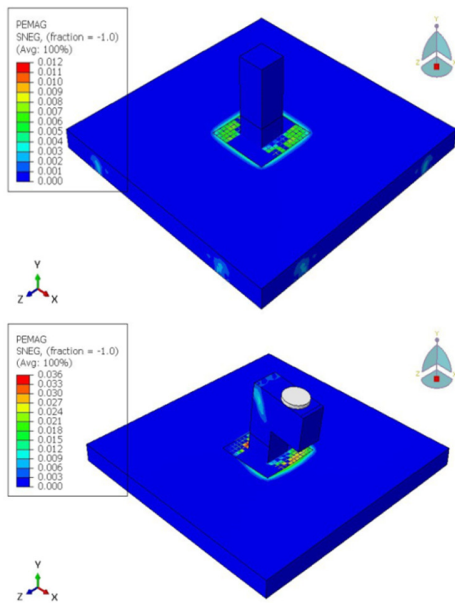
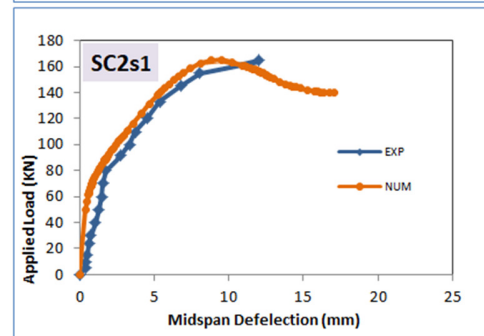
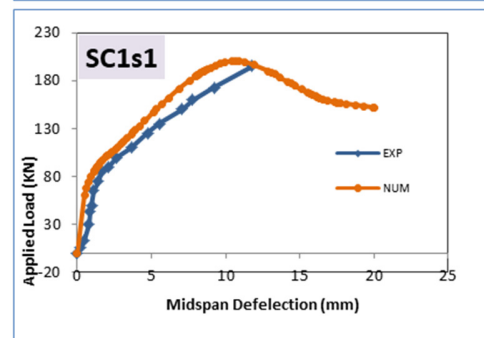
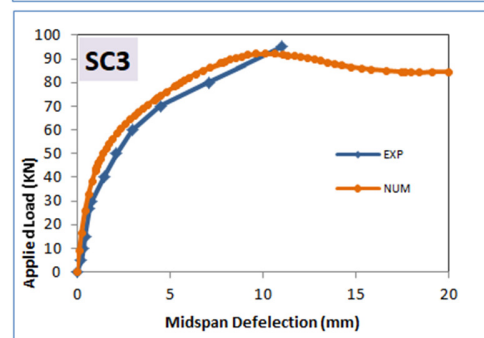
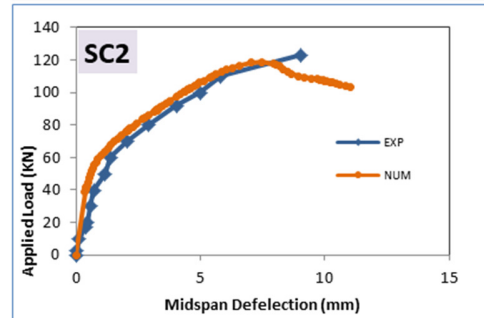
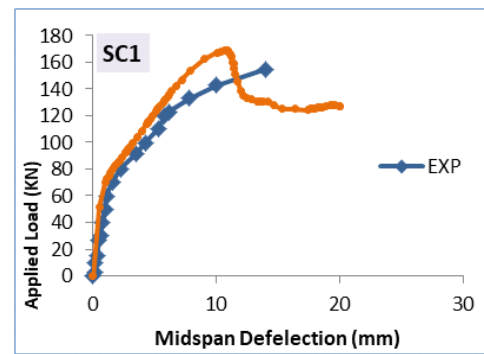


Fig. 10. Steel collars.

VI. LOAD DEFLECTION AND MODE FAILUER OF ANALYSIS

This part examines the simulated finite element models. The load set was gradually applied at the same level as that of the experimental test. The acquired failure mode of the slabs from FEM at the final stage of loading before the solution diverges. To validate the created finite element models, the failure load and the load-deflection relationship of the modeling were compared with the corresponding test results. Figure 11 presents the comparison between the experimental data and the outcomes derived from the model. The first crack originates adjacent to the perimeter of the column on the tensile side in the concrete structure with a longitudinal shape.



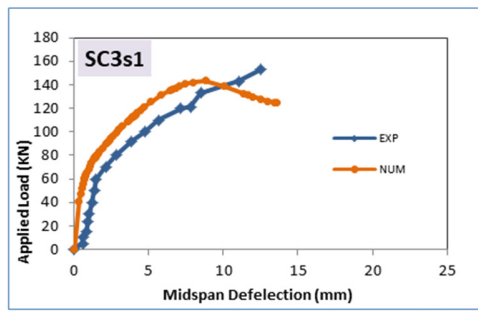


Fig. 11. Experimental and numerical ultimate load-deflection relationship of slabs.

After the first crack, several longitudinal cracks emerged parallel to the flexural bars (Figure 12). With the increasing

load, the concrete slab experienced the emergence of transverse cracks that were eventually interconnected with the longitudinal fissures. Furthermore, radial cracks initiated from the center of the slab extended towards the edges and corners. This pattern of cracking indicates the progressive failure and redistribution of stresses within the slab under the applied load. Shear cracks with irregular circular shapes appeared at the bottom of the column on the tension side when it reached its collapse load. In the reinforced specimens, the number of cracks exceeded that of the reference slab due to the load reaching elevated magnitudes. At SC1 and SC1s1, where the punching shear strength reached its maximum values, the failure area perimeter expanded. Table IV displays the analytical results.

TABLE IV. ANALYTICAL RESULTS.

Specimens ID	P_u (kN) Exp.	Δ_u (mm) Exp.	P_u (kN) Num.	Δ_u (mm) Num.	P_{uExp}/P_{uNum}	Failure mode
SC1	155	12.5	164	11.18	0.94	Punching shear
SC2	123	10	120	8.23	1.03	Punching shear
SC3	95	9	92	10.16	1.03	Punching shear
SC1s1	196	12	200	10.19	0.98	Punching shear
SC2s1	165	13	166	10.65	0.99	Punching shear
SC3s1	153	12.5	145	10.06	1.05	Punching shear

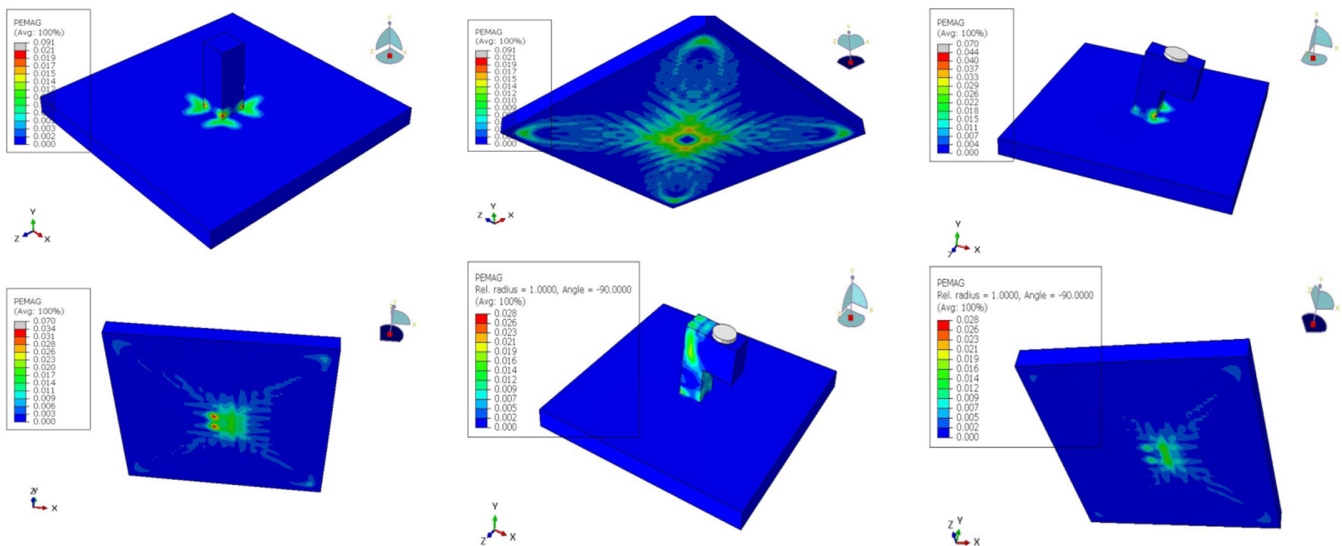


Fig. 12. Failure modes from molding slabs.

VII. CONCLUSION

This work experimented with flat slabs under eccentric load. The proposed economical solution to maintain and rehabilitate buildings against punching shear is the use of steel collars. Other studies examine strengthening punching shear under concentric load but this work simulates other loads and the unbalance moment effect on the building. The observations of this study provide evidence of the deleterious effects of the eccentric loading and unbalanced moments on the ultimate load of a slab with the absence of steel collars. The ultimate load capacity dropped by 26% to 60% (a value that fully illustrates their relevance to adopting steel collaring strengthening

methods), providing compelling arguments for using such methods to attenuate these effects. Furthermore, the numerical approach validation involving finite element analysis proved that the analytical approach is useful and reliable in estimating the punching shear strength of the slabs. Several key conclusions regarding the strengthening of slab-column connections and the effect of eccentricity load were derived:

- The stiff behavior of the load deflection relationship at a slab-column strengthening was compared with specimens of the unstrengthening cross section.
- The steel collar strengthening method was efficient in extending the perimeter of the critical shear so that the

failure mechanism did not change, but just shifted away from the column's face.

- When strengthening the slab-column using steel collar, the collapse did not happen directly, but gradually by increasing cracks width. The perimeter of the failure zone increases when steel collar is used, therefore, the shear strength increases.
- The specimens that were tested with eccentric load have a lower ultimate load capacity on the account of the influence of unbalanced moments.
- Most cracks of the punching shear occur at one side more than at the other side in specimens with eccentricity.

Recommendation: More parameters should be studied under eccentric load, such as compressive strength of concrete, thickness of slab, and the addition of carbon fiber sheets.

REFERENCES

- [1] P. G. Fernández, A. Marí, and E. Oller, "Theoretical prediction of the punching shear strength of concrete flat slabs under in-plane tensile forces," *Engineering Structures*, vol. 229, Feb. 2021, Art. no. 111632, <https://doi.org/10.1016/j.engstruct.2020.111632>.
- [2] A. Ngab and M. S. Shahin, "A Simple Equation for Predicting the Punching Shear Capacity of Normal and High Strength Concrete Flat Plates," *International Journal of Engineering Research & Technology*, vol. 10, no. 3, pp. 678–688, Mar. 2021, <https://doi.org/10.13140/RG.2.2.10182.80961>.
- [3] A. A. Jaafer, R. AL-Shadidi, and S. L. Kareem, "Enhancing the Punching Load Capacity of Reinforced Concrete Slabs Using an External Epoxy-Steel Wire Mesh Composite," *Fibers*, vol. 7, no. 8, Aug. 2019, Art. no. 68, <https://doi.org/10.3390/fib7080068>.
- [4] D. Vargas, E. O. L. Lantsoght, and A. S. Genikomsou, "Flat Slabs in Eccentric Punching Shear: Experimental Database and Code Analysis," *Buildings*, vol. 12, no. 12, Dec. 2022, Art. no. 2092, <https://doi.org/10.3390/buildings12122092>.
- [5] B. Binici and O. Bayrak, "Punching Shear Strengthening of Reinforced Concrete Flat Plates Using Carbon Fiber Reinforced Polymers," *Journal of Structural Engineering*, vol. 129, no. 9, pp. 1173–1182, Sep. 2003, [https://doi.org/10.1061/\(ASCE\)0733-9445\(2003\)129:9\(1173\)](https://doi.org/10.1061/(ASCE)0733-9445(2003)129:9(1173)).
- [6] A. Hameed, H. Husain, and M. Al-Sherrawi, "Analysis of Corner Column-Slab Connections in Concrete Flat Plates," *East African Scholars Journal of Engineering and Computer Sciences*, vol. 2, no. 1, pp. 37–46, Jan. 2019.
- [7] M. H. Makhlof, G. Ismail, A. H. Abdel Kreem, and M. I. Badawi, "Investigation of transverse reinforcement for R.C flat slabs against punching shear and comparison with innovative strengthening technique using FRP ropes," *Case Studies in Construction Materials*, vol. 18, Jul. 2023, Art. no. e01935, <https://doi.org/10.1016/j.cscm.2023.e01935>.
- [8] K. F. El-Kashif, E. A. Ahmed, and H. M. Salem, "Experimental investigation of strengthening slab-column connections with CFRP fan," *Ain Shams Engineering Journal*, vol. 10, no. 3, pp. 639–650, Sep. 2019, <https://doi.org/10.1016/j.asej.2019.02.005>.
- [9] H. S. Askar, "Usage of prestressed vertical bolts for retrofitting flat slabs damaged due to punching shear," *Alexandria Engineering Journal*, vol. 54, no. 3, pp. 509–518, Sep. 2015, <https://doi.org/10.1016/j.aej.2015.05.013>.
- [10] B. Q. Abdulrahman and O. Q. Aziz, "Strengthening RC flat slab-column connections with FRP composites: A review and comparative study," *Journal of King Saud University - Engineering Sciences*, vol. 33, no. 7, pp. 471–481, Nov. 2021, <https://doi.org/10.1016/j.jksues.2020.07.005>.
- [11] A. Salama, "Punching shear behavior Of GFRP-RC edge slab column connections with and without shear stirrups reinforcement," Ph.D. dissertation, University of Sherbrooke, Sherbrooke, Canada, 2019.
- [12] M. Lapi, A. P. Ramos, and M. Orlando, "Flat slab strengthening techniques against punching-shear," *Engineering Structures*, vol. 180, pp. 160–180, Feb. 2019, <https://doi.org/10.1016/j.engstruct.2018.11.033>.
- [13] S. Kadhim and H. Ammash, "Steel Stiffeners for Enhancement of Slab-Column Connections," *Al-Qadisiyah Journal for Engineering Sciences*, vol. 12, no. 4, pp. 199–206, Dec. 2019, <https://doi.org/10.30772/qjes.v12i4.621>.
- [14] A. A. Abdulhussein and M. H. Al-Sherrawi, "Experimental study on strengthening punching shear in concrete flat plates by steel collars," *AIP Conference Proceedings*, vol. 2651, no. 1, Mar. 2023, Art. no. 020026, <https://doi.org/10.1063/5.0130802>.
- [15] H. K. Ammash, S. S. Kadhim, and M. K. Dhahir, "Repairing half-loaded flat slabs against punching shear using steel stiffeners," *Case Studies in Construction Materials*, vol. 16, Jun. 2022, Art. no. e01032, <https://doi.org/10.1016/j.cscm.2022.e01032>.
- [16] K. F. El-Kashif, E. A. Ahmed, and H. M. Salem, "Experimental investigation of strengthening slab-column connections with CFRP fan," *Ain Shams Engineering Journal*, vol. 10, no. 3, pp. 639–650, Sep. 2019, <https://doi.org/10.1016/j.asej.2019.02.005>.
- [17] M. Zahid and S. Al-Zaidee, "Validated Finite Element Modeling of Lightweight Concrete Floors Stiffened and Strengthened with FRP," *Engineering, Technology & Applied Science Research*, vol. 13, no. 4, pp. 11387–11392, Aug. 2023, <https://doi.org/10.48084/etasr.6055>.
- [18] A. E. Salama, M. Hassan, and B. Benmokrane, "Effectiveness of Glass Fiber-Reinforced Polymer Stirrups as Shear Reinforcement in Glass Fiber-Reinforced Polymer- Reinforced Concrete Edge Slab-Column Connections," *Structural Journal*, vol. 116, no. 5, pp. 97–112, Sep. 2019, <https://doi.org/10.14359/51716757>.
- [19] A. A. Abdulhussein and M. H. Al-Sherrawi, "Experimental and Numerical Analysis of the Punching Shear Resistance Strengthening of Concrete Flat Plates by Steel Collars," *Engineering, Technology & Applied Science Research*, vol. 11, no. 6, pp. 7853–7860, Dec. 2021, <https://doi.org/10.48084/etasr.4497>.
- [20] Widiyanto, "Rehabilitation of Reinforced Concrete Slab-column Connections for Two-way Shear," Ph.D. dissertation, The University of Texas at Austin, Austin TX, USA, 2006.
- [21] ACI Committee 318, *ACI CODE-318-19: Building Code Requirements for Structural Concrete and Commentary*. Farmington Hills, MI, USA: ACI, 2019.
- [22] *Standard Test Method for Compressive Strength of Cylindrical Concrete Specimens*, West Conshohocken, PA, USA: ASTM International, 2019.
- [23] *ASTM C496/C496M-17: Standard Test Method for Splitting Tensile Strength of Cylindrical Concrete Specimens*. West Conshohocken, PA, USA: ASTM International, 2017.
- [24] *ASTM C78/C78M-21, Standard Test Method for Flexural Strength of Concrete (Using Simple Beam with Third-Point Loading)*, West Conshohocken, PA, USA: ASTM International, 2021.
- [25] Z. A. Neamah and M. A. Al-Ramahee, "Punching shear strength of flat slab strengthened with reinforced concrete column capital under bi-axial loading," *IOP Conference Series: Materials Science and Engineering*, vol. 1067, no. 1, Oct. 2021, Art. no. 012005, <https://doi.org/10.1088/1757-899X/1067/1/012005>.
- [26] A. M. Abdel-Rahman, N. Z. Hassan, and A. M. Soliman, "Punching shear behavior of reinforced concrete slabs using steel fibers in the mix," *HBRC Journal*, vol. 14, no. 3, pp. 272–281, Dec. 2018, <https://doi.org/10.1016/j.hbrj.2016.11.001>.
- [27] M. H. Makhlof, G. Ismail, A. H. Abdel Kreem, and M. I. Badawi, "Investigation of transverse reinforcement for R.C flat slabs against punching shear and comparison with innovative strengthening technique using FRP ropes," *Case Studies in Construction Materials*, vol. 18, Jul. 2023, Art. no. e01935, <https://doi.org/10.1016/j.cscm.2023.e01935>.
- [28] A. H. Jasim and H. K. Ammash, "Effect of using column capital on the punching shear strength of flat slab-edge column connection under eccentric loading," *Journal of Physics: Conference Series*, vol. 1895, no. 1, Feb. 2021, Art. no. 012060, <https://doi.org/10.1088/1742-6596/1895/1/012060>.